RESEARCH ARTICLE

Utility of cardiac magnetic resonance feature tracking strain assessment in chronic thromboembolic pulmonary hypertension for prediction of REVEAL 2.0 high risk status

Kai'En Leong[1,2] | Luke Howard[3,4] | Francesco Lo Giudice[3,5] | Rachel Davies[3] | Gulammehdi Haji[3] | Simon Gibbs[4,6] | Deepa Gopalan[1,6,7]

[1]Department of Radiology, Imperial College Healthcare NHS Trust/ Hammersmith Hospital, London, UK

[2]Department of Cardiology, The Royal Melbourne Hospital, Victoria, Australia

[3]National Pulmonary Hypertension Service, Imperial College Healthcare NHS Trust, London, UK

[4]National Heart & Lung Institute, Imperial College London, London, UK

[5]Department of Cardiology, Imperial College Healthcare NHS Trust/ Hammersmith Hospital, London, UK

[6]Imperial College London, London, UK

[7]Department of Radiology, Cambridge University Hospitals NHS Trust, Cambridge, UK

Correspondence
Deepa Gopalan, Department of Radiology, Imperial College NHS Trust/ Hammersmith Hospital, DuCane Rd, London W12 0HS, UK.
Email: d.gopalan@nhs.net

Abstract

Chronic thromboembolic pulmonary hypertension may be cured by pulmonary endarterectomy (PEA). Thromboembolic disease distribution/PEA success primarily determines prognosis but risk scoring criteria may be adjunctive. Right ventriculoarterial (RV-PA) and ventriculoatrial (RV-right atrium [RA]) coupling may be evaluated by cardiac MRI (CMR) feature tracking deformation/strain assessment. We characterized biatrial and biventricular CMR feature tracking (FT) strain parameters following PEA and tested the ability of CMR FT to identify REVEAL 2.0 high-risk status. We undertook a retrospective single-center cross-sectional study of patients ($n = 57$) who underwent PEA (2015–2020). All underwent pre and postoperative catheterization and CMR. Pulmonary arterial hypertension validated risk scores were calculated. Significant postoperative improvements were observed in mean pulmonary artery pressure (mPAP) (pre-op 45 ± 11 mmHg vs. post-op 26 ± 11 mmHg; $p < 0.001$) and PVR however a large proportion had residual pulmonary hypertension (45%; mPAP ≥ 25 mmHg). PEA augmented left heart filling with left ventricular end diastolic volume index and left atrial volume index increment. Left ventricular ejection fraction was unchanged postoperatively but LV global longitudinal strain improved (pre-op median -14.2% vs. post-op -16.0%; $p < 0.001$). Right ventricular (RV) geometry and function also improved with reduction in RV mass. Most had uncoupled RV-PA relationships which recovered (pre-op right ventricular free wall longitudinal strain $-13.2 \pm 4.8\%$, RV stroke volume/right ventricular end systolic volume ratio 0.78 ± 0.53 vs. post-op $-16.8 \pm 4.2\%$, 1.32 ± 0.55; both $p < 0.001$). Postoperatively, there were six REVEAL 2.0 high-risk patients, best predicted by impaired RA strain which was superior to traditional volumetric

Deepa Gopalan and Simon Gibbs are co-senior authors.

parameters (area under the curve [AUC] 0.99 vs. RVEF AUC 0.88). CMR deformation/strain evaluation can offer insights into coupling recovery; RA strain may be an expeditious surrogate for the more laborious REVEAL 2.0 score.

KEYWORDS

feature tracking (CMR-FT), pulmonary endarterectomy, strain, ventriculoarterial coupling, ventriculoatrial coupling

INTRODUCTION

Chronic thromboembolism is an underrecognized cause of pulmonary hypertension (PH). Arising as a late consequence of acute pulmonary embolism (PE) in approximately 4%,[1] chronic thromboembolic pulmonary hypertension (CTEPH) may occur without prior acute PE history in up to 25% of patients.[2] Classified as "Group 4" in PH guidelines,[3] the overall full incidence (including undiagnosed cases) of CTEPH is estimated at 3–5 cases per 100,000 population/year.[1]

CTEPH patients develop progressive pulmonary vascular remodeling with resultant pulmonary vascular resistance (PVR) elevation.[4] Untreated, eventual right ventricular (RV) failure confers a risk of premature mortality.[5]

Pulmonary endarterectomy (PEA) is the sole curative treatment for CTEPH and has excellent success performed in expert centers.[6,7] Appropriate patient selection is crucial with the central disease most surgically amenable, while distal disease may be treated with balloon pulmonary angioplasty or targeted medical therapy with riociguat.[3,7,8]

While PEA results are principally favorable in selected patients, a significant proportion have residual PH (mean pulmonary artery pressure [mPAP] ≥ 25 mmHg)[6] and there is no consensus regarding the optimal investigative regimen to detect this.[3]

Unlike pulmonary arterial hypertension (PAH) with multiple risk scores (namely the REVEAL 2.0,[9] French PH network [FPHN],[10] comparative prospective registry of newly initiated therapies for pulmonary hypertension (COMPERA)[11] and Swedish PAH registry [SPAHR][12] criteria) validated for the prediction of transplant-free survival, anatomical distribution of disease still remains the central consideration in CTPEH.[3] However, the mutual prognostic applicability of these PAH risk criteria in CTEPH has been suggested by some recent data.[13–15]

Beyond distribution/nature of the thromboembolic disease, other clinical features and hemodynamic findings[6,7,16,17] such as functional class, comorbidities, and notably, an early postoperative (PEA) invasive

mPAP ≥ 38 mmHg and PVR ≥ 425 dynes (5.3 WU) are associated with worse survival in CTEPH.[6] There are, however, limited imaging prognostic parameters.

Contemporarily, there is growing interest in strain imaging with deformation assessment offering additive diagnostic and prognostic value in various pathologies.[18,19] However, most data relate to the echocardiographic (TTE) speckle tracking technique, although cardiac MRI (CMR) feature tracking (FT) strain appears reasonably concordant.[20] There is a current paucity of literature specifically examining CMR FT strain in CTEPH.

The relationship between the right ventricle (RV) and its load has been described by the paradigm of "coupling."[21–23] Succinctly, the latter term describes energy transfer efficiency, and RV-PA coupling has an estimated (unitless) normal range of 1.0–2.0 to express matching of ventricular contractility to arterial afterload.[24] While principally assessed by invasive pressure–volume catheterization, there are emerging data for the role of CMR[22,25–27] in its evaluation. The majority of interest has centered on the RV-PA relationship but there is increasing recognition of the significance of the RV-right atrium (RA) relationship[28] which may be evaluated by RA deformation imaging and have prognostic importance in pulmonary hypertension.[26,29]

In this work, we sought to characterize biatrial and biventricular CMR FT deformation parameters in CTEPH patients following PEA, and correlate the former with invasive hemodynamics to examine changes in ventricular coupling. Various risk scoring criteria were then applied, to test the ability of CMR FT to identify REVEAL 2.0 high-risk status.

METHODS

Design

This was a retrospective cross-sectional study with all CTEPH patients from January 1, 2015 to July 31, 2020

screened for eligibility. Consecutive patients were included if they underwent PEA at an affiliated expert institution and had pre- and postoperative CMR and cardiac catheterization performed by our service. Patients were excluded if there were incomplete/missing paired (pre- and postoperative) investigations.

CMR

All patients underwent CMR on a 1.5 T Siemens Aera scanner using a 32-channel phased array surface coil as part of routine care pre- and post-PEA.

Cine imaging was performed with breath-held steady-state free precession sequences to derive contiguous parallel short axis slices of the RV and LV from base to apex, as well as standard long axis slices of the heart. Slice prescription parameters were 8 mm thickness/2 mm gap for short axis imaging with 1.5–2 mm in-plane spatial resolution, 33–45 ms temporal resolution, and 25–30 reconstructed cardiac phases.

CMR postprocessing and FT strain

CMR studies were analyzed using Circle Cardiovascular Imaging software (CVI42, version 5.12.1). Volumetric analysis was performed as per current guidelines.[30]

Right ventricular mass was determined from the short axis stack using the end-diastolic phase, with the inclusion of papillary muscle mass by blood pool thresholding.[31] The interventricular septal mass was assigned to the left ventricle.[31,32]

Although a detailed description of the concepts of deformation is beyond this work's scope but is available in various review literature,[33,34] strain (ε) is a dimensionless parameter reflecting change in length and given by $\varepsilon = (L - L_0)/L_0$, with L_0 denoting the original and L the final length. Accordingly, with systolic longitudinal strain, a negative value indicates myocardial shortening and a positive value lengthening.

FT strain assessment was also performed using CVI42. Endocardial contours were traced using automatic detection by "3 clicks" (two at the base, one at the apex) definition of chamber extent. Minor manual endocardial adjustment was applied as required. Epicardial boundaries were traced manually. Chamber borders were traced at ventricular end-diastole to define strain zero baseline (R–R gating), and longitudinal strain quantification was performed automatically by the software using a deformable myocardial model.[20,35–37] LA strain and LV global longitudinal strain (GLS) were computed using the 4 and 2 chamber cines while only the 4 chamber cine was used for RA strain and RV strain.

With regard to the RV, only the free wall endo- and epicardial borders were traced to derive the RV free wall longitudinal strain (RVFWLS), with tracing and deformation of the septum designated to the LV.

Three repeat tracings and measurements of peak biatrial reservoir and peak systolic biventricular strain were performed, and the average was recorded.

Twenty percent of patients were randomly selected for atrial and ventricular strain measurement by a second investigator to determine interobserver variability. Intraobserver variability was assessed with one investigator re-measuring atrial and ventricular strain after a 1-month interval.

Right heart catheterization

Patients were allowed only oral clear fluids before catheterization. Vascular access was gained via right internal jugular (ultrasound-guided) or occasionally right antecubital venous puncture. A Swan-Ganz catheter was used for all pressure measurements. Pulmonary arterial wedge pressure (PAWP) tracings were obtained at end-expiration (mean of three tracings in sinus rhythm or five in atrial fibrillation/AF). Cardiac output (CO) measurements were made using the thermodilution or Fick method. PVR (Wood units/WU) was calculated by (mPAP−mPAWP)/CO.

Distribution of disease and surgical clearance success

Surgical notes were reviewed to determine the Jamieson classification[38,39] of thromboembolic disease for each lung—Type I with central thromboemboli, Type II with intimal thickening, fibrous webs, and bands, Type III with segmental and subsegmental branch occlusions, and Type IV with very distal thromboemboli/microvascular disease. Subjective clearance success of each lung (as per the operating surgeon's opinion) was also recorded and scored with three clearance grades—1 = excellent, 2 = good, and 3 = limited. A total "CTEPH score" was calculated by summing bilateral Jamieson grades and surgical success for each lung so that a score of 4 would indicate bilateral Type 1 central disease with bilateral excellent clearance.

Risk category assessment

To assess the change in risk profiles following PEA, all patients had pre- and postoperative risk scores calculated using the REVEAL 2.0,[9] French PH network (FPHN),[10] COMPERA[11] and Swedish PAH registry (SPAHR)[12] criteria (Supporting Information: Table 1).

Input parameters for risk score calculation were extracted from discharge summaries and relevant contemporaneous investigations of the final preoperative and first postoperative inpatient workup admissions.

REVEAL 2.0 was chosen as the final risk scoring system for evaluation against CMR due to its inclusion of the greatest number of prognostic parameters (Supporting Information: Table 1) and its derivation population being the largest.[40]

Statistical analysis

Continuous normal data are presented as mean (± 1 SD). Non-normal data are presented as median (interquartile range). Continuous data were compared with the (paired) two-tailed Student's t-test or (paired) Wilcoxon test for normal and non-normal data respectively. Categorical variables are displayed as n (%) and differences were assessed using Fisher's exact test. Correlation analysis was performed using Pearson's correlation coefficient or Spearman's rank test where data was non-normal. Intraclass correlation coefficient (ICC) estimates for inter- and intraobserver variability in strain assessment were calculated. Univariate and multivariate stepwise logistic regression was performed to identify CMR parameters that predicted REVEAL 2.0 high-risk status. Receiver operating characteristic (ROC) curves with area under the curve (AUC) values were used to compare the discriminative ability of the various parameters and the optimal cut-points were defined by the Youden index. A $p \leq 0.05$ was considered statistically significant.

RESULTS

CMR FT strain reproducibility: Inter- and intraobserver variability

Measurement of FT biatrial and biventricular strain was feasible in all patients. There was excellent inter- and intraobserver agreement. Interobserver ICC were 0.98 for RA (0.89–0.99), 1.0 for LA (0.98–1.0), 0.99 for RV (0.96–1.0), and 0.97 for LV (0.90–0.99).

Intraobserver ICC for the RA, LA, RV, and LV were 0.99 (0.98–1.0), 0.99 (0.98–1.0), 0.99 (0.97–1.0), and 0.97 (0.89–0.99) respectively.

Patients

A total of 97 patients were identified. Forty were excluded due to incomplete pre and/or postoperative investigations with the final cohort comprising 57 patients (Supporting Information: Figure 1).

Patients were aged 56 ± 14 years and balanced between genders. Nineteen percent of all patients did not have an acute PE history but all were anticoagulated with warfarin the most common agent. At the time of surgery, Jamieson Type I disease was infrequent in either lung (21% right lung, 14% left lung) with a median total CTEPH score of 8 (Table 1). CMR was performed 197 ± 86 days preoperatively and 111 (98–145) days postoperatively. Catheterization was typically undertaken during the same admission and performed 199 ± 87 days preoperatively and 111 (97–148) days postoperatively.

Postoperatively, there was significant improvement in 6-min walk distance (6MWD) and functional class, with a concurrent reduction in BNP levels. Only five patients (9%) remained on PDE5i compared to 18 (32%; $p = 0.003$) preoperatively (Table 1).

Invasive hemodynamics

There was significant improvement in all hemodynamic parameters postoperatively however a large proportion of patients had residual PH (45%; mPAP $\geq$ 25 mmHg) and elevated PVR (35%; PVR > 3WU) (Table 2).

CMR

Preoperatively, all patients had small underfilled left hearts relative to the right with reduced LV mass (normal reference range male LV mass index $74 \pm 8.5 \text{ g/m}^2$; female $63 \pm 7.5 \text{ g/m}^2$).[32] Left ventricular ejection fraction (LVEF) was preserved in all but longitudinal function assessed by GLS was impaired (Table 3).

All patients had dilated impaired right hearts with RVFWLS and RVEF commensurately reduced. Using the volumetric approximation for RV-PA coupling (RV stroke volume [SV]/right ventricular end systolic volume [RVESV] ratio),[41,42] most had "uncoupled" relationships. RV mass index was significantly increased in all (normal

TABLE 1 Baseline patient characteristics and postoperative change in medical therapy

	Pre-op (n = 57)	Post-op (n = 57)	p Value
Age (years)	56 ± 14	-	-
Gender	31 M (54%)	-	-
	26 F (46%)	-	-
BMI (kg/m²)	29.1 (25.1-34.4)	-	-
RL Jamieson Type 1	12 (21%)	-	-
LL Jamieson Type 1	8 (14%)	-	-
Total CTEPH score	8 (6-8.25)	-	-
Acute PE history	46 (81%)	-	-
Functional class			
I–II	6 (11%)	41 (72%)	**<0.001**
III–IV	51 (89%)	16 (28%)	**<0.001**
6 MWD (m)	251 ± 115	311 ± 130	**0.003**
eGFR by CKD-EPI (ml/ min/1.73 m2)	74 ± 14	76 ± 14	NS
Anticoagulation			
Warfarin	27 (47%)	26 (46%)	NS
Apixaban	5 (9%)	6 (11%)	NS
Rivaroxaban	22 (39%)	19 (33%)	NS
Edoxaban	1 (2%)	2 (4%)	NS
LMWH	2 (4%)	4 (7%)	NS
Medical therapy			
Nil else (only anticoagulation)	25 (44%)	33 (58%)	NS
Diuretics	21 (37%)	17 (30%)	NS
MRA	9 (16%)	10 (18%)	NS
PDE5i	18 (32%)	5 (9%)	**0.003**
ETRA	3 (5%)	0	NS
Riociguat	1 (2%)	4 (7%)	NS
Supplemental oxygen therapy	6 (11%)	3 (5%)	NS
BNP (ng/L)	171 (81-599)	69 (32-145)	**<0.001**
CMR-surgery interval (days)	197 ± 86	111 (98-145)	-
Catheterization-surgery interval (days)	199 ± 87	111 (97-148)	-

Note: Bold values are statistically significant at *p* < 0.05.

Abbreviations: 6 MWD, 6-min walk distance; BNP, B-type natriuretic peptide; CMR, cardiac magnetic resonance (study); CKD-EPI, chronic kidney disease-epidemiology collaboration; eGFR, estimated glomerular filtration rate; ETRA, endothelin receptor antagonist; LL, left lung; LMWH, low molecular weight heparin; MRA, mineralocorticoid receptor antagonist; PDE5i, phosphodiesterase type 5 inhibitor; post-op, postoperative; pre-op, preoperative; RL, right lung.

TABLE 2 Postoperative change in invasive hemodynamic parameters of all patients

	Pre-op (n = 57)	Post-op (n = 57)	p Value
mPAP (mmHg)	45 ± 11	26 ± 11	**<0.001**
Postoperative mPAP (mmHg)			
<20	-	14 (25%)	-
20–24	-	17 (30%)	-
≥25	-	26 (45%)	-
mPAWP (mmHg)	11 ± 4	11 ± 4	NS
mRAP (mmHg)	10 ± 5	7 ± 4	**<0.001**
PVR (WU)	9.1 (6.1–12.4)	2.5 (1.7–3.8)	**<0.001**
Postoperative PVR (WU)			
<1.5	-	10 (18%)	-
1.5–3	-	27 (47%)	-
>3	-	20 (35%)	-
Cardiac index (L/min/m²)	2.1 ± 0.7	2.7 ± 0.7	**<0.001**
SvO₂ (%)	62.8 ± 9.2	70.1 ± 7.8	**<0.001**
Systolic BP (mmHg)	126 ± 20	125 ± 18	NS
HR (bpm)	77 ± 14	76 ± 12	NS

Note: All patients underwent catheterization. Bold values are statistically significant at *p* < 0.05.

Abbreviations: BP, blood pressure; HR, heart rate; mPAP, mean pulmonary artery pressure; mPAWP, mean pulmonary arterial wedge pressure; mRAP, mean right atrial pressure; post-op, postoperative; pre-op, preoperative; PVR, pulmonary vascular resistance; SvO₂, mixed venous oxygen saturation.

reference range male RV mass index 34 ± 7 g/m²; female 28 ± 5 g/m²).[31]

Following pulmonary endarterectomy, enhanced left heart filling was associated with increased left ventricular end diastolic volume index and left atrial volume index (LAVi). No significant change in LVEF was seen but LV GLS improved postoperatively. Right heart geometry and function improved with reduction in RV mass (Table 3).

Please see Figures 1–3 for illustrative case examples.

Correlation analysis

Pre- and postoperative CMR and catheterization studies were analyzed (114 data sets; 57 pre-op and post-op pairs).

All RA peak strain and RVFWLS correlation relationships were highly significant (RA strain-PVR ρ −0.34 [−0.50 to −0.1], RA strain-mPAP ρ −0.31 [−0.47 to

TABLE 3 Postoperative change in CMR parameters of all patients

	Pre-op ($n = 57$)	Post-op ($n = 57$)	p Value
LVEDVi (ml/m²), all patients	57 ± 16	63 ± 13	**0.003**
Male ($n = 31$)	62 ± 16	68 ± 14	**0.041**
Females ($n = 26$)	52 ± 14	57 ± 9	**0.034**
LVESVi (ml/m²)	21 (16–28)	23 (18–28)	NS
LV SVi (ml/m²)	35 ± 10	39 ± 8	**0.002**
LV mass index (g/m²), all patients	55 (49–66)	61 (54–67)	**0.012**
Male ($n = 31$)	63 (55–74)	65 (61–68)	NS
Females ($n = 26$)	50 ± 12	55 ± 11	**0.030**
LVEF (%)	60 ± 10	63 ± 9	NS
LV GLS (%)	−14.2 (−16.2 to −11.1)	−16.0 (−17.9 to −14.5)	**<0.001**
LAVi (ml/m²)	32 (23–39)	34 (28–44)	**<0.001**
Peak LA strain (%)	22.3 (15.9–28.5)	25.8 (18.5–30.3)	**0.024**
RVEDVi (ml/m²)	113 ± 36	78 ± 26	**<0.001**
RVESVi (ml/m²)	71 ± 34	37 ± 22	**<0.001**
RV SVi (ml/m²)	42 ± 14	41 ± 9	NS
RV mass index (g/m²), all patients	43 (32–49)	30 (27–33)	**<0.001**
Male ($n = 31$)	45 ± 13	34 ± 11	**<0.001**
Female ($n = 26$)	38 (29–44)	29 (24–32)	**<0.001**
RVEF (%)	40 ± 15	55 ± 10	**<0.001**
RVFWLS (%)	−13.2 ± 4.8	−16.8 ± 4.2	**<0.001**
RAVi (ml/m²)	73 ± 35	49 ± 20	**<0.001**
Peak RA strain (%)	16.7 (10.1–24.6)	18.3 (15.7–25.3)	NS
LA/RA volume ratio	0.56 ± 0.32	0.83 ± 0.36	**<0.001**
LVEDV/RVEDV ratio	0.56 ± 0.22	0.85 ± 0.20	**<0.001**
LVESV/RVESV ratio	0.39 ± 0.21	0.73 ± 0.25	**<0.001**
RV SV/RVESV ratio	0.78 ± 0.53	1.32 ± 0.55	**<0.001**
MPA diameter index (mm/m²)	17.9 (15.5–19.6)	15.1 (13.8–17.8)	**<0.001**

Note: All patients underwent CMR. Bold values are statistically significant at $p < 0.05$.

Abbreviations: CMR, cardiac MRI; GLS, global longitudinal strain; LAVi, left atrial volume index; LV, left ventricular; LVEDVi, left ventricular end diastolic volume index; LVEF, left ventricular ejection fraction; MPA, main pulmonary artery; post-op, postoperative; pre-op, preoperative; RA, right atrium; RV, right ventricular; RVESV, right ventricular end systolic volume; RVFWLS, right ventricular free wall longitudinal strain, SV, stroke volume.

−0.14], RVFWLS-mPAP ρ 0.54 [0.39–0.66], RVFWLS-PVR ρ 0.57 [0.43–0.68]; all $p < 0.001$) (Figures 4 and 5).

The strongest RA strain associations were with mean right atrial pressure (ρ −0.43 [−0.57 to −0.27]) and RV SV/RVESV ratio (ρ 0.55 [0.41–0.67]) (Figure 5). RVFWLS was more closely related to RV SV/RVESV ratio (ρ −0.74 [−0.81 to −0.64]). A similar magnitude correlation was seen for the RVFWLS-RVEF relationship (ρ −0.74 [−0.82 to −0.65]) (Figure 4).

In both genders (Supporting Information: Figures 2 and 3), reduction in RV mass index was significantly correlated (all $p \leq 0.05$) with postoperative

improvements in RVEF (male ρ −0.79 [−0.87 to −0.68]; female ρ −0.69 [−0.81 to −0.52]), RVFWLS (male ρ 0.58 [0.39 to 0.72]; female ρ 0.59 [0.38 to 0.74]) and RV SV/RVESV ratio (male ρ −0.79 [−0.87 to −0.68]; female ρ −0.69 [−0.81 to −0.52]). RA strain was also negatively correlated with RV mass (male ρ −0.39 [−0.58 to −0.15], $p = 0.002$; female ρ −0.35 [−0.57 to −0.08], $p = 0.011$) although the strength of association was weaker compared to RV parameters.

Lastly, RV mass index was significantly correlated with PVR in both males (ρ 0.68 [0.52–0.80]; $p < 0.001$) and females (ρ 0.69 [0.51–0.81]; $p < 0.001$) with
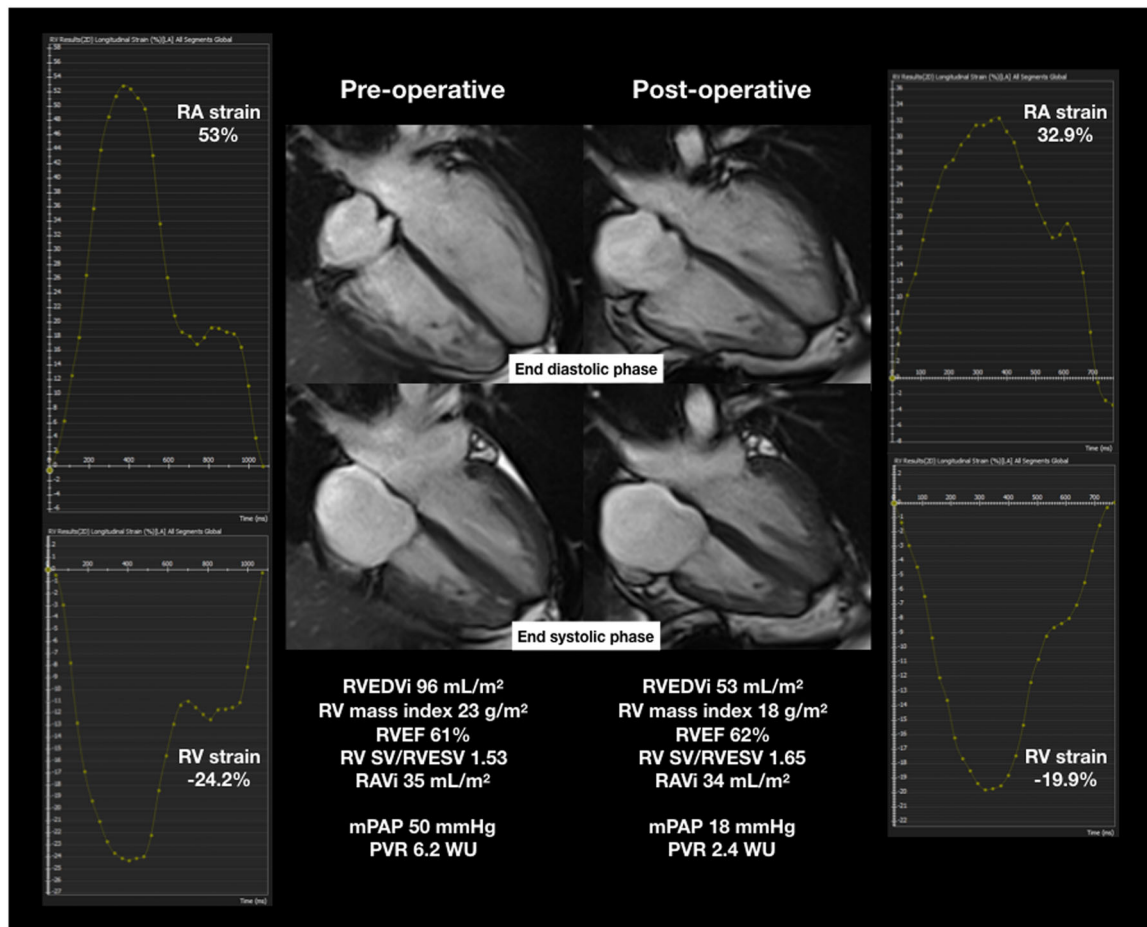
FIGURE 1 Thirty-year-old female; compensated right heart with right ventriculoarterial (RV-PA) coupling maintained preoperatively and augmented right atrium (RA) compliance (preoperative RA strain 53%)

RV mass increasing with PVR (Supporting Information: Figure 4).

Risk score assessment

With REVEAL 2.0 as the reference, the FPHN score overestimated risk with a larger number of patients classified as high-risk pre and postoperatively whereas the COMPERA and SPAHR scores underestimated risk with fewer patients in the high-risk category (Figure 6).

In the entire cohort of patients ($n = 57$), there were only 6 (11%) classified as REVEAL 2.0 high risk postoperatively.

Clinical characteristics and key investigations of postoperative high-risk patients are summarized in Table 4. All were male, aged 59 ± 16 years. Postoperative 6 MWD were markedly reduced at 101 ± 19 m and BNP levels significantly elevated at 252 (152–372) ng/L.

Postoperative mPAP and PVR remained substantially elevated at 39 ± 11 mmHg and 5.0 ± 1.6 WU, respectively.

RV-PA relationships were uncoupled as indicated by an RV SV/RVESV ratio of 0.70 ± 0.37 and RVFWLS of $-9.1 \pm 3.3\%$. Reflecting more advanced dysfunction, RV-RA relationships were uncoupled as well with a peak RA strain of $6.4 \pm 3.4\%$.

Prediction of REVEAL 2.0 high risk

Impaired peak RA strain was the best predictor of a REVEAL 2.0 high-risk classification (AUC 0.99; $p < 0.001$) with a peak RA strain cut point of ≤14.9% having 100% sensitivity and 86% specificity (Table 5 and Figure 7). RVFWLS was also an excellent predictor of high-risk status (AUC 0.97) and was superior to RVESVi (AUC 0.90) and RVEF (AUC 0.88).

Notably, peak LA strain reduction showed very strong predictive ability (AUC 0.97) for identifying REVEAL 2.0 high-risk status as did LV GLS (AUC 0.90). With multivariate logistic regression, peak RA strain was the only independent predictor of
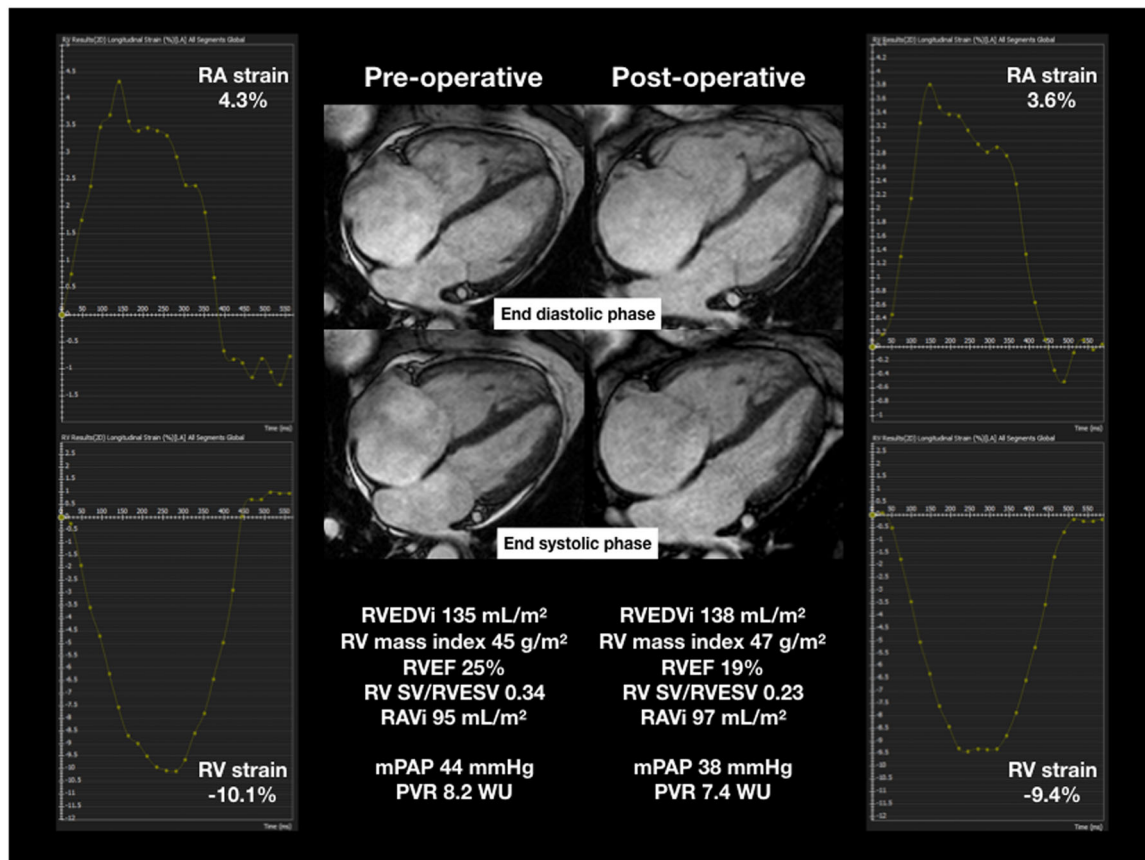
FIGURE 2 Fifty-seven-year-old male; fully decompensated right heart with uncoupled right ventriculoarterial (RV-PA) and ventriculoatrial (RV-RA) relationships. Postoperative REVEAL 2.0 high-risk status. Pre- and postoperative four chamber cine video clips with RA strain overlay in animation supplement.

REVEAL 2.0 high-risk status (Supporting Information: Table 2).

DISCUSSION

In this work, we have characterized biatrial peak reservoir and biventricular peak systolic strain in CTEPH patients pre- and post-PEA. Additionally, we have shown that RA strain best predicted REVEAL 2.0 high-risk status and was superior to traditional volumetric parameters.

Corresponding with prior data,[6] a significant proportion of patients in this study had postoperative residual PH (mPAP ≥ 25 mmHg). While CTEPH outcome is mainly determined by thromboembolic disease distribution/operative success and invasive hemodynamics remain essential in postoperative risk assessment, it is accepted that prognostication should utilize a multi-parametric approach[14] (e.g., REVEAL 2.0) rather than a single criterion (i.e., mPAP or PVR

alone). The main drawback would be the requirement for an extensive testing panel to derive a risk score.

Postoperatively, six patients in the entire cohort (11%) were classified as REVEAL 2.0 high risk which confers a 12-month > 10% mortality risk in PAH patients.[9] These patients were accurately identified by severe RA strain impairment representing late-stage RV dysfunction with ventriculoatrial decoupling. Notably, their corresponding postoperative invasive hemodynamic parameters showed significantly elevated mPAP and PVR at 39 ± 11 mmHg and 5.0 ± 1.6 WU, respectively. Prior data[6] have indicated this magnitude of postoperative mPAP and PVR elevation to be associated with mortality risk. This would suggest prognostic applicability of the REVEAL 2.0 score in post-PEA patients and support the routine assessment of peak RA strain with its excellent REVEAL 2.0 high-risk predictive ability although larger prospective studies are necessary to validate this finding.

Additionally, the majority of patients in the entire cohort had normal postoperative LA sizes. Similarly, LVEF was preserved. Marked reductions in peak LA
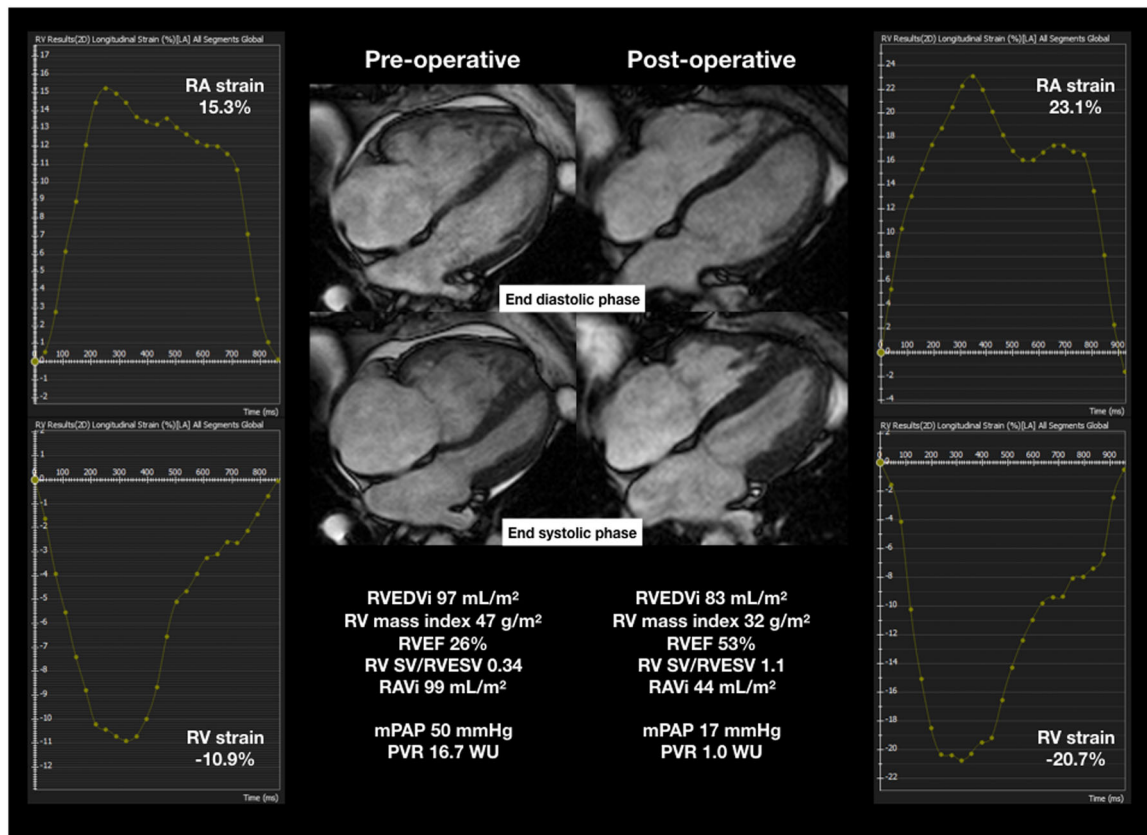
FIGURE 3 Forty-eight-year-old male; uncoupled right ventriculoarterial (RV-PA) and ventriculoatrial (RV-right atrium [RA]) relationships preoperatively with restoration post pulmonary endarterectomy. Pre- and postoperative four chamber cine video clips with RA strain overlay in animation supplement.
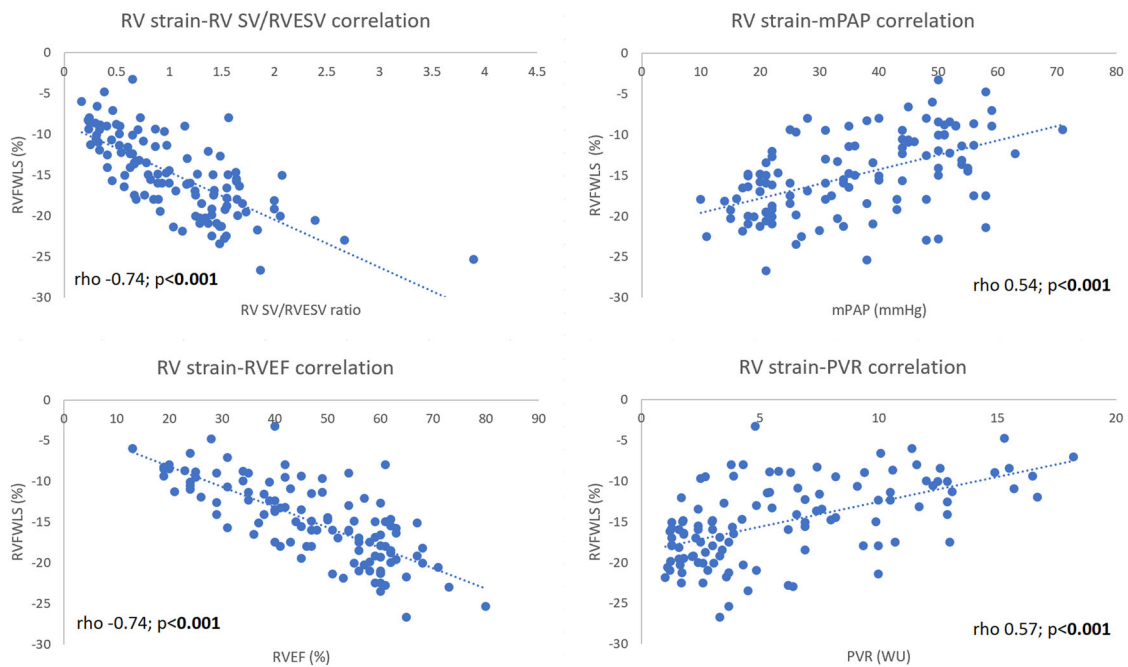
FIGURE 4 RV strain correlation (RV SV/RVESV, RVEF, mPAP, PVR) scatter plots. Strong correlation between RV strain-RVEF and moderate strength RV strain association with invasive hemodynamics. mPAP, mean pulmonary artery pressure; PVR, pulmonary vascular resistance; RV, right ventricular; RVESV, right ventricular end systolic volume; SV, stroke volume.
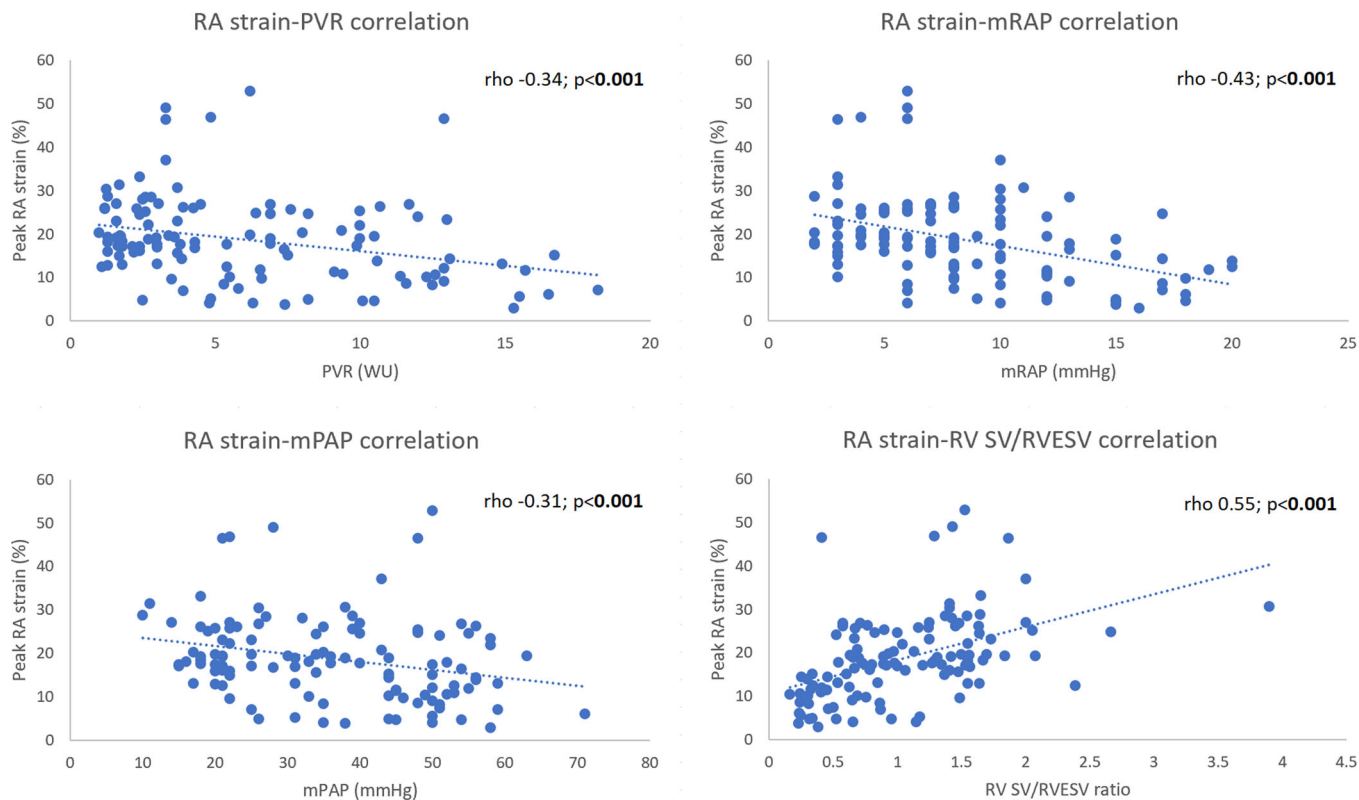
FIGURE 5 RA strain correlation (PVR, mRAP, mPAP, RV SV/RVESV) scatter plots. Significant but weak strength association between RA strain and invasive hemodynamics. mPAP, mean pulmonary artery pressure; mRAP, mean right atrial pressure; PVR, pulmonary vascular resistance; RA, right atrium; RVESV, right ventricular end systolic volume; RV, right ventricular; SV, stroke volume.
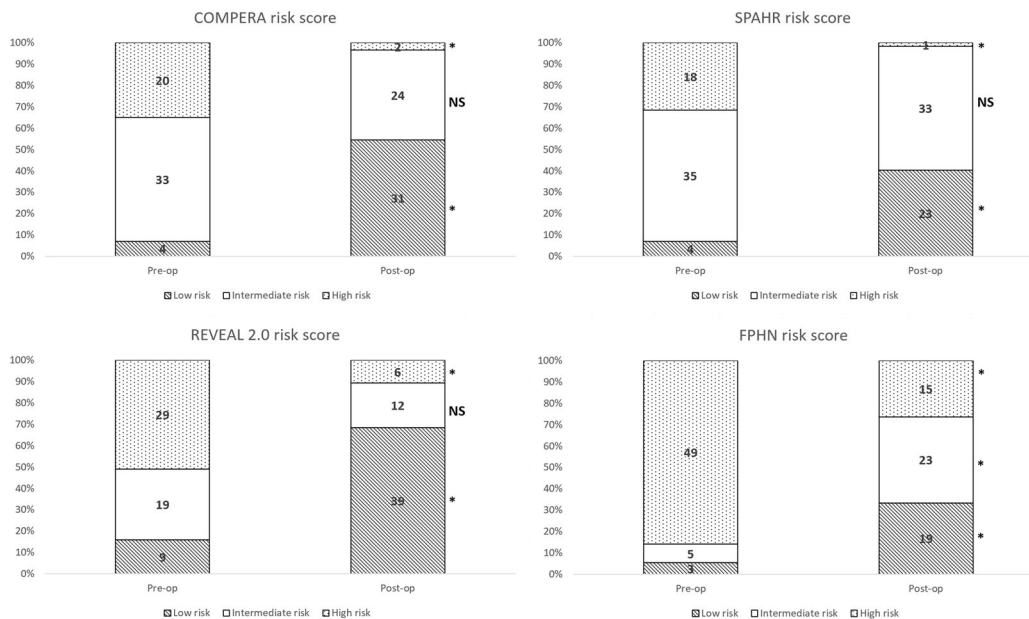
FIGURE 6 Different risk category proportions dependent on the scoring criteria used. Using REVEAL 2.0 as the reference, the FPHN score overestimated risk with a larger number of patients classified as high-risk pre and postoperatively whereas the COMPERA and SPAHR scores underestimated risk with fewer patients in the high-risk category. *Statistically significant difference ($p < 0.001$) in pre versus postoperative risk category. COMPERA, comparative prospective registry of newly initiated therapies for pulmonary hypertension; FPHN, French PH network. SPAHR, Swedish PAH registry.

TABLE 4 Clinical characteristics, invasive hemodynamics, and CMR parameters of postoperative REVEAL 2.0 high risk patients

	Postoperative REVEAL 2.0 high risk patients ($n = 6$)
Age (years)	59 ± 16
Gender	6 M (100%)
BMI (kg/m^2)	31.8 ± 6.2
eGFR by CKD-EPI (ml/min/ 1.73 m^2)	67 ± 19
Post-op BNP (ng/L)	252 (152–372)
6 MWD (m)	101 ± 19
Anticoagulation	
Warfarin	3
Rivaroxaban	2
LMWH	1
Medical therapy	
Nil else (only anticoagulation)	0
Diuretics	5
MRA	4
PDE5i	2
Riociguat	1
Supplemental oxygen therapy	1
Postoperative invasive hemodynamics	
mPAP (mmHg)	39 ± 11
mPAWP (mmHg)	13 ± 2
mRAP (mmHg)	12 ± 5
PVR (WU)	5.0 ± 1.6
Cardiac index (L/min/m^2)	2.4 ± 0.5
SvO$_2$ (%)	59.5 ± 8.3
Postoperative CMR parameters	
LVEDVi (ml/m^2)	68 ± 9
LV mass index (g/m^2)	67 ± 10
LVEF (%)	48 ± 11
LV GLS (%)	-10.0 ± 3.7
LAVi (ml/m^2)	52 ± 17
Peak LA strain (%)	8.7 ± 6.1
RVEDVi (ml/m^2)	115 ± 42
RV mass index (g/m^2)	44 ± 16
RVEF (%)	39 ± 14
RVFWLS (%)	-9.1 ± 3.3

TABLE 4 (Continued)

	Postoperative REVEAL 2.0 high risk patients ($n = 6$)
RAVi (ml/m^2)	85 ± 26
Peak RA strain (%)	6.4 ± 3.4
RV SV/RVESV ratio	0.70 ± 0.37

Abbreviations: 6 MWD, 6-min walk distance; BNP, B-type natriuretic peptide; CKD-EPI, chronic kidney disease-epidemiology collaboration; eGFR, estimated glomerular filtration rate; GLS, global longitudinal strain; LMWH, low molecular weight heparin; LAVi, left atrial volume index; LV, left ventricular; LVEDVi, left ventricular end diastolic volume index; LVEF, left ventricular ejection fraction; mPAP, mean pulmonary artery pressure; mPAWP, mean pulmonary arterial wedge pressure; mRAP, mean right atrial pressure; PVR, pulmonary vascular resistance; RA, right atrium; RV, right ventricular; RVESV, right ventricular end systolic volume; RVFWLS, right ventricular free wall longitudinal strain; SV, stroke volume.

strain and LV GLS were able to predict REVEAL 2.0 high risk status, which reflects the importance of ventricular interdependence with worsening right ventricular geometry, function, and septal motion negatively impacting left ventricular filling mechanics.[43,44] This adverse physiology is again not immediately apparent if solely utilizing volumetric measures (LVEF and LAVi) for left heart assessment and CMR FT strain may hence present additive diagnostic and prognostic value.

Current guidelines[3] do not suggest a postoperative imaging strategy but with deformation assessment, CMR may be valuable as the first line postoperative imaging modality, offering more precise insights into understanding RV-PA and RV-RA coupling physiology as compared to sole utilization of traditional volumetric imaging.

Using the reference standard of pressure-volume catheterization to assess RV-PA coupling by end-systolic elastance/arterial elastance ratio (Ees/Ea), Tello et al.[25] demonstrated that CMR FT RVFWLS had a good ability for identifying RV-PA uncoupling (Ees/Ea < 0.805 mmHg/ml) with a cut-point of > −15.29% showing 70% sensitivity and 89% specificity. In this work, most patients had postoperative restoration of RV-PA coupling with significant improvements in their RVFWLS.

With riociguat a therapeutic option for patients with significant symptomatic residual PH post-PEA,[3,45,46] deformation imaging may be of value in monitoring early response/improvements in RV-PA coupling and be more sensitive than RVEF to subtle change, akin to the role of LV GLS in assessing for cancer-therapy related cardiac dysfunction.[47] In a small ($n = 27$) mixed PAH/CTEPH cohort with mild PH, Murata et al.[48]

TABLE 5 CMR predictors of REVEAL 2.0 high-risk status

CMR parameter	ROC curve AUC (95% CI)	p Value	Cut point for REVEAL 2.0 high risk	Sensitivity (95% CI)	Specificity (95% CI)	+LR	−LR
LV SVi (ml/m²)	0.79 (0.66–0.89)	**<0.001**	≤33	67% (22–96)	82% (69–92)	3.8	0.4
LV GLS (%)	0.90 (0.79–0.96)	**<0.001**	>−14.5	83% (36–100)	82% (69–92)	4.7	0.2
Peak LA strain (%)	0.97 (0.89–1.00)	**<0.001**	≤16.8	100% (54–100)	86% (74–94)	7.3	0.0
RVEDVi (ml/m²)	0.85 (0.73–0.93)	**<0.001**	>85	83% (36–100)	75% (60–86)	3.3	0.2
RVESVi (ml/m²)	0.90 (0.79–0.96)	**<0.001**	>42	83% (36–100)	80% (67–90)	4.3	0.2
RVEF (%)	0.88 (0.76–0.95)	**<0.001**	≤49	83% (36–100)	78% (65–89)	3.9	0.2
RVFWLS (%)	0.97 (0.89–1.00)	**<0.001**	>−15	100% (54–100)	82% (69–92)	5.7	0.0
RAVi (ml/m²)	0.94 (0.84–0.99)	**<0.001**	>58	83% (36–100)	82% (69–92)	4.7	0.2
Peak RA strain (%)	0.99 (0.92–1.00)	**<0.001**	≤14.9	100% (54–100)	86% (74–94)	7.3	0.0
LVEDV/RVEDV ratio	0.82 (0.70–0.91)	**0.003**	≤0.75	67% (22–96)	78% (65–89)	3.1	0.4
RV SV/RVESV ratio	0.89 (0.78–0.96)	**<0.001**	≤0.95	83% (36–100)	78% (65–89)	3.9	0.2

Note: Greatest AUC (0.99) of peak RA strain for REVEAL 2.0 high-risk status, exceeding RVEF (AUC 0.88). Bold values are statistically significant at $p < 0.05$.

Abbreviations: AUC, area under the curve; CI, confidence interval; CMR, cardiac magnetic resonance (study); GLS, global longitudinal strain; LV, left ventricular; ROC, receiver operating characteristic; RA, right atrium; RV, right ventricular; RVESV, right ventricular end systolic volume; RVFWLS, right ventricular free wall longitudinal strain; SV, stroke volume.
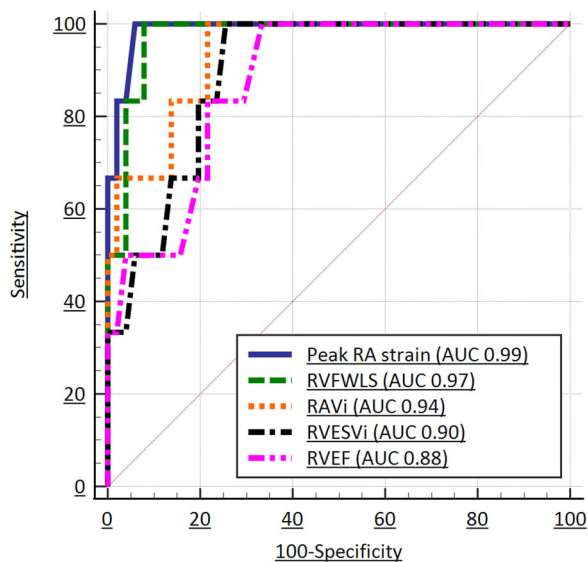
FIGURE 7 ROC curve comparison of CMR predictors of REVEAL 2.0 high risk status. Largest AUC (0.99) with peak RA strain and smallest with RVEF (AUC 0.88). AUC, area under the curve; CMR, cardiac magnetic resonance (study); RA, right atrium; ROC, receiver operating characteristic.

showed riociguat improved TTE RV strain in patients with preserved longitudinal RV function (normal RVS' and TAPSE pre and post-riociguat).

There is growing recognition of the importance of RA function in the pathophysiology of PH.[49,50] In a canine PH model from PA banding, early compensation was characterized by preserved systolic but impaired RV diastolic function, and increased RA distensibility (increased reservoir strain).[51] The augmented RA distensibility would be counterpoise to RV diastolic dysfunction and avert clinical heart failure. With increasing PH chronicity and severity, RV-PA then RV-RA uncoupling would ensue with diminution of RA reservoir function resulting in symptoms.[23,26]

This was illustrated in further work by Tello et al.[26] who showed impairment of RA phasic function correlating mainly with RV lusitropic dysfunction (RVEDP and end-diastolic elastance) rather than RV contractility. This finding was attributed to the majority of their cohort having uncoupled RV-PA relationships indicating the limit of compensatory RV contractile augmentation (by increased RV mass) had been

exceeded and RA phasic dysfunction represented a later stage in disease trajectory with worsening RV diastolic dysfunction.[21] This is congruent with our correlation analyses demonstrating the volumetric approximation of RV-PA coupling (RV SV/RVESV ratio) having a stronger relationship with RVFWLS than RA strain. This is also reflected in our observations regarding the stronger correlation between RV mass index, PVR, and RV SV/RVESV (early increment in RV mass to augment/match contractility with increased afterload and maintain coupling) and weaker RV mass correlation with RA strain (later stage disease).

Various RA reservoir strain cut-points have been proposed to coincide with different stages of RV maladaptation[26,50] with RV-RA decoupling occurring at a RA reservoir strain of approximately <16%. Pre and postoperatively, a large proportion of patients had preserved RV-RA coupling (pre-op median 16.7% increasing to a post-op median 18.3%; $p =$ NS). However, the six postoperative REVEAL 2.0 high-risk patients had a markedly reduced RA strain of $6.4 \pm 3.4\%$ suggesting advanced RV dysfunction/RV-RA uncoupling despite endarterectomy and underpins the strong diagnostic performance of RA strain in predicting REVEAL 2.0 high-risk status.

CONCLUSION

Significant improvement in cardiac hemodynamics, geometry, and function may be achieved post pulmonary endarterectomy, however, a sizeable proportion of patients have residual pulmonary hypertension and PVR elevation.

It is accepted that risk assessment is best served by utilization of multiple criteria. While not fully validated for application in CTEPH patients, postoperative REVEAL 2.0 high-risk status was accurately predicted by markedly reduced RA strain which corresponds with late stage right ventricular dysfunction and ventriculoatrial decoupling. As such, RA strain may be a more expeditiously obtained surrogate of REVEAL 2.0 high risk which requires an extensive battery of tests to compute. The incorporation of deformation assessment may enhance the prognostic utility of CMR in CTEPH and aid in the refinement of risk stratification.

LIMITATIONS

This was a single-center retrospective study of a relatively small size ($n = 57$) with a large number of patients excluded ($n = 40$) due to incomplete paired

investigations. All patients were alive at 12 months, however, no additional clinical/functional data have been collected at this time point for purposes of this study. It would be crucial to show mortality association with postoperative REVEAL 2.0 high-risk status, thus validating the utility of RA strain. However, this study of 57 patients (with only six postoperative REVEAL 2.0 high risk) was underpowered to examine this. Using the older iteration of REVEAL, Benza et al.[14] recorded only 24 deaths in a much larger cohort of 243 CTEPH patients, with mortality associated with a higher REVEAL risk score. Reflecting the retrospective nature of this study and our current real-world practice, a significant time interval existed between preoperative investigations and PEA with the possibility for deterioration in hemodynamics and imaging parameters. Catheterization and CMR parameters at first postoperative follow-up were used in this study with the possibility for further improvement with later testing; however current literature suggests similarity/stability in tested metrics over the medium term.[6,52] We acknowledge that deformation assessment by TTE speckle tracking may be more advantageous than CMR FT due to TTE ubiquity and ease of access, lower cost, shorter scan duration, and superior temporal resolution. However, we sought to highlight the comprehensive utility of CMR in CTEPH, where management is typically undertaken at tertiary centers with the routine performance of CMR for (gold standard) RV evaluation and RA FT strain assessment may be retrospectively and conveniently measured without the need for additional MRI sequences. Lastly, atrial strain was not assessed using a dedicated atrial feature tracking algorithm but rather by a ventricular algorithm from a specific vendor.

AUTHOR CONTRIBUTIONS

Kai'En Leong, Luke Howard, Deepa Gopalan, and Simon Gibbs contributed to conception and design of the study. Kai'En Leong organized the database. Kai'En Leong and Deepa Gopalan performed the image analysis. Kai'En Leong performed the statistical analysis. Kai'En Leong wrote the first draft of the manuscript. Luke Howard, Francesco Lo Giudice, Gulammehdi Haji, and Rachel Davies wrote sections of the manuscript. All authors contributed to manuscript revision, read, and approved the submitted version.

CONFLICT OF INTEREST

The authors declare no conflict of interest.

ETHICS STATEMENT

This study was approved by the Heath Research Authority (HRA) and NHS Research Ethics Service (REC) (IRAS ID 280472/Protocol 20HH5838) with waivers of informed consent due to the retrospective design.

ORCID

Kai'En Leong http://orcid.org/0000-0001-5556-9825

REFERENCES

1. Gall H, Hoeper MM, Richter MJ, Cacheris W, Hinzmann B, Mayer E. An epidemiological analysis of the burden of chronic thromboembolic pulmonary hypertension in the USA, Europe and Japan. Eur Respir Rev. 2017;26(143):160121.
2. Pepke-Zaba J, Delcroix M, Lang I, Mayer E, Jansa P, Ambroz D, Treacy C, D'Armini AM, Morsolini M, Snijder R, Bresser P, Torbicki A, Kristensen B, Lewczuk J, Simkova I, Barberà JA, de Perrot M, Hoeper MM, Gaine S, Speich R, Gomez-Sanchez MA, Kovacs G, Hamid AM, Jaïs X, Simonneau G. Chronic thromboembolic pulmonary hypertension (CTEPH): results from an international prospective registry. Circulation. 2011;124(18):1973–81.
3. Galiè N, Humbert M, Vachiery JL, Gibbs S, Lang I, Torbicki A, Simonneau G, Peacock A, Vonk Noordegraaf A, Beghetti M, Ghofrani A, Gomez Sanchez MA, Hansmann G, Klepetko W, Lancellotti P, Matucci M, McDonagh T, Pierard LA, Trindade PT, Zompatori M, Hoeper M. 2015 ESC/ERS Guidelines for the diagnosis and treatment of pulmonary hypertension: The Joint Task Force for the Diagnosis and Treatment of Pulmonary Hypertension of the European Society of Cardiology (ESC) and the European Respiratory Society (ERS): endorsed by: Association for European Paediatric and Congenital Cardiology (AEPC), International Society for Heart and Lung Transplantation (ISHLT). Eur Respir J. 2015;46(4):903–75.
4. Lang IM, Madani M. Update on chronic thromboembolic pulmonary hypertension. Circulation. 2014;130(6):508–18.
5. Hoeper MM, Mayer E, Simonneau G, Rubin LJ. Chronic thromboembolic pulmonary hypertension. Circulation. 2006;113(16):2011–20.
6. Cannon JE, Su L, Kiely DG, Page K, Toshner M, Swietlik E, Treacy C, Ponnaberanam A, Condliffe R, Sheares K, Taboada D, Dunning J, Tsui S, Ng C, Gopalan D, Screaton N, Elliot C, Gibbs S, Howard L, Corris P, Lordan J, Johnson M, Peacock A, MacKenzie-Ross R, Schreiber B, Coghlan G, Dimopoulos K, Wort SJ, Gaine S, Moledina S, Jenkins DP, Pepke-Zaba J. Dynamic risk stratification of patient long-term outcome after pulmonary endarterectomy: results from the United Kingdom National Cohort. Circulation. 2016;133(18):1761–71.
7. Jenkins D, Madani M, Fadel E, D'Armini AM, Mayer E. Pulmonary endarterectomy in the management of chronic thromboembolic pulmonary hypertension. Eur Respir Rev. 2017;26(143):160111.
8. Jenkins D. Pulmonary endarterectomy: the potentially curative treatment for patients with chronic thromboembolic pulmonary hypertension. Eur Respir Rev. 2015;24(136):263–71.
9. Benza RL, Gomberg-Maitland M, Elliott CG, Farber HW, Foreman AJ, Frost AE, McGoon MD, Pasta DJ, Selej M, Burger CD, Frantz RP. Predicting survival in patients with pulmonary arterial hypertension: the REVEAL risk score calculator 2.0 and comparison with ESC/ERS-Based risk assessment strategies. Chest. 2019;156(2):323–37.
10. Boucly A, Weatherald J, Savale L, Jaïs X, Cottin V, Prevot G, Picard F, de Groote P, Jevnikar M, Bergot E, Chaouat A, Chabanne C, Bourdin A, Parent F, Montani D, Simonneau G, Humbert M, Sitbon O. Risk assessment, prognosis and guideline implementation in pulmonary arterial hypertension. Eur Respir J. 2017;50(2):1700889.
11. Hoeper MM, Kramer T, Pan Z, Eichstaedt CA, Spiesshoefer J, Benjamin N, Olsson KM, Meyer K, Vizza CD, Vonk-Noordegraaf A, Distler O, Opitz C, Gibbs J, Delcroix M, Ghofrani HA, Huscher D, Pittrow D, Rosenkranz S, Grünig E. Mortality in pulmonary arterial hypertension: prediction by the 2015 European pulmonary hypertension guidelines risk stratification model. Eur Respir J. 2017;50(2):1700740.
12. Kylhammar D, Kjellström B, Hjalmarsson C, Jansson K, Nisell M, Söderberg S, Wikström G, Rådegran G. A comprehensive risk stratification at early follow-up determines prognosis in pulmonary arterial hypertension. Eur Heart J. 2018;39(47):4175–81.
13. Sandqvist A, Kylhammar D, Bartfay SE, Hesselstrand R, Hjalmarsson C, Kavianipour M, Nisell M, Rådegran G, Wikström G, Kjellström B, Söderberg S. Risk stratification in chronic thromboembolic pulmonary hypertension predicts survival. Scand Cardiovasc J. 2021;55(1):43–9.
14. Benza RL, Farber HW, Frost A, Grünig E, Hoeper MM, Busse D, Meier C, Nikkho S, Ghofrani HA. REVEAL risk score in patients with chronic thromboembolic pulmonary hypertension receiving riociguat. J Heart Lung Transplant. 2018;37(7):836–43.
15. Benza RL, Farber HW, Frost AE, Ghofrani HA, Corris PA, Brockmann B, Nikkho S, Meier C, Hoeper MM. Validation of REVEAL risk score calculator 2.0 in patients with CTEPH in the Phase III CHEST Study. J Heart Lung Transplant. 2020;39(4):S32–S3.
16. Delcroix M, Lang I, Pepke-Zaba J, Jansa P, D'Armini AM, Snijder R, Bresser P, Torbicki A, Mellemkjaer S, Lewczuk J, Simkova I, Barberà JA, de Perrot M, Hoeper MM, Gaine S, Speich R, Gomez-Sanchez MA, Kovacs G, Jaïs X, Ambroz D, Treacy C, Morsolini M, Jenkins D, Lindner J, Dartevelle P, Mayer E, Simonneau G. Long-term outcome of patients with chronic thromboembolic pulmonary hypertension: results from an International Prospective Registry. Circulation. 2016;133(9):859–71.
17. Madani MM, Auger WR, Pretorius V, Sakakibara N, Kerr KM, Kim NH, Fedullo PF, Jamieson SW. Pulmonary endarterectomy: recent changes in a single institution's experience of more than 2,700 patients. Ann Thorac Surg. 2012;94(1):97–103.
18. Ayach B, Fine NM, Rudski LG. Right ventricular strain: measurement and clinical application. Curr Opin Cardiol. 2018;33(5):486–92.
19. Potter E, Marwick TH. Assessment of left ventricular function by echocardiography: the case for routinely adding global

longitudinal strain to ejection fraction. JACC Cardiovasc Imaging. 2018;11(2 Pt 1):260–74.

20. Vo HQ, Marwick TH, Negishi K. MRI-derived myocardial strain measures in normal subjects. JACC Cardiovasc Imaging. 2018;11(2 Pt 1):196–205.

21. Vonk Noordegraaf A, Westerhof BE, Westerhof N. The relationship between the right ventricle and its load in pulmonary hypertension. J Am Coll Cardiol. 2017;69(2): 236–43.

22. Tello K, Dalmer A, Axmann J, Vanderpool R, Ghofrani HA, Naeije R, Roller F, Seeger W, Sommer N, Wilhelm J, Gall H, Richter MJ. Reserve of right ventricular-arterial coupling in the setting of chronic overload. Circ Heart Fail. 2019; 12(1):e005512.

23. Lang IM, Binder T. Right atrial strain is a surrogate of coupling in the right heart. Eur Heart J Cardiovasc Imaging. 2020;21(8):863–4.

24. Sunagawa K, Maughan WL, Sagawa K. Optimal arterial resistance for the maximal stroke work studied in isolated canine left ventricle. Circ Res. 1985;56(4):586–95.

25. Tello K, Dalmer A, Vanderpool R, Ghofrani HA, Naeije R, Roller F, Seeger W, Wilhelm J, Gall H, Richter MJ. Cardiac magnetic resonance imaging-based right ventricular strain analysis for assessment of coupling and diastolic function in pulmonary hypertension. JACC cardiovasc imaging. JACC Cardiovasc Imaging. 2019;12(11 Pt 1):2155–64.

26. Tello K, Dalmer A, Vanderpool R, Ghofrani HA, Naeije R, Roller F, Seeger W, Wiegand M, Gall H, Richter MJ. Right ventricular function correlates of right atrial strain in pulmonary hypertension: a combined cardiac magnetic resonance and conductance catheter study. Am J Physiol Heart Circ Physiol. 2020;318(1):H156–64.

27. Waziri F, Ringgaard S, Mellemkjær S, Bøgh N, Kim WY, Clemmensen TS, Hjortdal VE, Nielsen SL, Poulsen SH. Long-term changes of right ventricular myocardial deformation and remodeling studied by cardiac magnetic resonance imaging in patients with chronic thromboembolic pulmonary hypertension following pulmonary thromboendarterectomy. Int J Cardiol. 2020;300:282–8.

28. van Wezenbeek J, Kianzad A, van de Bovenkamp A, Wessels J, Mouratoglou SA, Braams NJ, Jansen S, Meulblok E, Meijboom LJ, Marcus JT, Vonk Noordegraaf A, José Goumans M, Jan Bogaard H, Handoko ML, de Man FS. Right atrial function is associated with RV diastolic stiffness: RA-RV interaction in pulmonary arterial hypertension. Eur Respir J. 2021;15:008726.

29. Alenezi F, Mandawat A, Il'Giovine ZJ, Shaw LK, Siddiqui I, Tapson VF, Arges K, Rivera D, Romano M, Velazquez EJ, Douglas PS, Samad Z, Rajagopal S. Clinical utility and prognostic value of right atrial function in pulmonary hypertension. Circ Cardiovasc Imaging. 2018;11(11):e006984.

30. Schulz-Menger J, Bluemke DA, Bremerich J, Flamm SD, Fogel MA, Friedrich MG, Kim RJ, von Knobelsdorff-Brenkenhoff F, Kramer CM, Pennell DJ, Plein S, Nagel E. Standardized image interpretation and post-processing in cardiovascular magnetic resonance—2020 update: Society for Cardiovascular Magnetic Resonance (SCMR): Board of Trustees Task Force on Standardized Post-Processing. J Cardiovasc Magn Reson. 2020;22(1):19.

31. Maceira AM, Prasad SK, Khan M, Pennell DJ. Reference right ventricular systolic and diastolic function normalized to age, gender and body surface area from steady-state free precession cardiovascular magnetic resonance. Eur Heart J. 2006;27(23): 2879–88.

32. Maceira AM, Prasad SK, Khan M, Pennell DJ. Normalized left ventricular systolic and diastolic function by steady state free precession cardiovascular magnetic resonance. J Cardiovasc Magn Reson. 2006;8(3):417–26.

33. Marwick TH. Measurement of strain and strain rate by echocardiography: ready for prime time? J Am Coll Cardiol. 2006;47(7):1313–27.

34. Gorcsan J, Tanaka H. Echocardiographic assessment of myocardial strain. J Am Coll Cardiol. 2011;58(14):1401–13.

35. Truong VT, Palmer C, Wolking S, Sheets B, Young M, Ngo T, Taylor M, Nagueh SF, Zareba KM, Raman S, Mazur W. Normal left atrial strain and strain rate using cardiac magnetic resonance feature tracking in healthy volunteers. Eur Heart J Cardiovasc Imaging. 2020;21(4):446–53.

36. Truong VT, Palmer C, Young M, Wolking S, Ngo T, Sheets B, Hausfeld C, Ornella A, Taylor MD, Zareba KM, Raman SV, Mazur W. Right atrial deformation using cardiovascular magnetic resonance myocardial feature tracking compared with two-dimensional speckle tracking echocardiography in healthy volunteers. Sci Rep. 2020;10(1):5237.

37. Bistoquet A, Oshinski J, Skrinjar O. Myocardial deformation recovery from cine MRI using a nearly incompressible biventricular model. Med Image Anal. 2008;12(1):69–85.

38. Jamieson SW. Pulmonary thromboendarterectomy. Heart. 1998;79(2):118–20.

39. Thistlethwaite PA, Mo M, Madani MM, Deutsch R, Blanchard D, Kapelanski DP, Jamieson SW. Operative classification of thromboembolic disease determines outcome after pulmonary endarterectomy. J Thorac Cardiovasc Surg. 2002;124(6):1203–11.

40. Galiè N, Channick RN, Frantz RP, Grünig E, Jing ZC, Moiseeva O, Preston IR, Pulido T, Safdar Z, Tamura Y, McLaughlin VV. Risk stratification and medical therapy of pulmonary arterial hypertension. Eur Respir J. 2019; 53(1):1801889.

41. Brewis M, Naeije R, Bellofiore A, Chesler N, Peacock A. Cardiac MRI derived right ventriculo-arterial coupling in pulmonary hypertension as a predictor of survival. Eur Respir J. 2014;44:P2300.

42. Vanderpool RR, Pinsky MR, Naeije R, Deible C, Kosaraju V, Bunner C, Mathier MA, Lacomis J, Champion HC, Simon MA. RV-pulmonary arterial coupling predicts outcome in patients referred for pulmonary hypertension. Heart. 2015;101(1):37–43.

43. Hardegree EL, Sachdev A, Fenstad ER, Villarraga HR, Frantz RP, McGoon MD, Oh JK, Ammash NM, Connolly HM, Eidem BW, Pellikka PA, Kane GC. Impaired left ventricular mechanics in pulmonary arterial hypertension: identification of a cohort at high risk. Circ Heart Fail. 2013;6(4):748–55.

44. Singh A, Kishiki K, Mor-Avi V, Maffessanti F, Gomberg-Maitland M, Lang RM, Addetia K. Abstract 19958: occult left atrial dysfunction in severe pulmonary arterial hypertension: a novel application of left atrial strain. Circulation. 2016;134 (Suppl_1):A19958.

Pulmonary Circulation Open Access

45. Simonneau G, D'Armini AM, Ghofrani HA, Grimminger F, Hoeper MM, Jansa P, Kim NH, Wang C, Wilkins MR, Fritsch A, Davie N, Colorado P, Mayer E. Riociguat for the treatment of chronic thromboembolic pulmonary hypertension: a long-term extension study (CHEST-2). Eur Respir J. 2015;45(5):1293–302.

46. Ghofrani HA, D'Armini AM, Grimminger F, Hoeper MM, Jansa P, Kim NH, Mayer E, Simonneau G, Wilkins MR, Fritsch A, Neuser D, Weimann G, Wang C, CHEST- Study G. Riociguat for the treatment of chronic thromboembolic pulmonary hypertension. N Engl J Med. 2013;369(4):319–29.

47. Plana JC, Galderisi M, Barac A, Ewer MS, Ky B, Scherrer-Crosbie M, Ganame J, Sebag IA, Agler DA, Badano LP, Banchs J, Cardinale D, Carver J, Cerqueira M, DeCara JM, Edvardsen T, Flamm SD, Force T, Griffin BP, Jerusalem G, Liu JE, Magalhães A, Marwick T, Sanchez LY, Sicari R, Villarraga HR, Lancellotti P. Expert consensus for multimodality imaging evaluation of adult patients during and after cancer therapy: a report from the American Society of Echocardiography and the European Association of Cardiovascular Imaging. Eur Heart J Cardiovasc Imaging. 2014;15(10):1063–93.

48. Murata M, Kawakami T, Kataoka M, Kohno T, Itabashi Y, Fukuda K. Riociguat, a soluble guanylate cyclase stimulator, ameliorates right ventricular contraction in pulmonary arterial hypertension. Pulm Circ. 2018;8(1):2045893217746111.

49. Querejeta Roca G, Campbell P, Claggett B, Solomon SD, Shah AM. Right atrial function in pulmonary arterial hypertension. Circ Cardiovasc Imaging. 2015;8(11):e003521.

50. Bhave NM, Visovatti SH, Kulick B, Kolias TJ, McLaughlin VV. Right atrial strain is predictive of clinical outcomes and invasive hemodynamic data in group 1 pulmonary arterial hypertension. Int J Cardiovasc Imaging. 2017;33(6):847–55.

51. Gaynor SL, Maniar HS, Bloch JB, Steendijk P, Moon MR. Right atrial and ventricular adaptation to chronic right ventricular pressure overload. Circulation. 2005;112(9 Suppl):I212–8.

52. D'Armini AM, Morsolini M, Mattiucci G, Grazioli V, Pin M, Valentini A, Silvaggio G, Klersy C, Dore R. Pulmonary endarterectomy for distal chronic thromboembolic pulmonary hypertension. J Thorac Cardiovasc Surg. 2014;148(3):1005–11.

SUPPORTING INFORMATION

Additional supporting information can be found online in the Supporting Information section at the end of this article.